

Catalysis Science & Technology

Accepted Manuscript



This is an *Accepted Manuscript*, which has been through the Royal Society of Chemistry peer review process and has been accepted for publication.

Accepted Manuscripts are published online shortly after acceptance, before technical editing, formatting and proof reading. Using this free service, authors can make their results available to the community, in citable form, before we publish the edited article. We will replace this *Accepted Manuscript* with the edited and formatted *Advance Article* as soon as it is available.

You can find more information about *Accepted Manuscripts* in the [Information for Authors](#).

Please note that technical editing may introduce minor changes to the text and/or graphics, which may alter content. The journal's standard [Terms & Conditions](#) and the [Ethical guidelines](#) still apply. In no event shall the Royal Society of Chemistry be held responsible for any errors or omissions in this *Accepted Manuscript* or any consequences arising from the use of any information it contains.

Cite this: DOI: 10.1039/c0xx00000x

www.rsc.org/xxxxxx

ARTICLE TYPE

A review of BiPO₄, a highly efficient oxyacid-type photocatalyst, for environmental applications

Chengsi Pan and Yongfa Zhu*^a*Received (in XXX, XXX) XthXXXXXXXXXX 20XX, Accepted Xth XXXXXXXXXXXX 20XX*

DOI: 10.1039/b000000x

Semiconductor photocatalysts for environmental applications has attracted much attention due to their ability to completely convert pollutants into CO₂ and H₂O. For simple and economical treatment, more efficient photocatalysts are highly desired compared to the widely used TiO₂. A nonmetallic oxyacid type photocatalyst, BiPO₄, was first discovered by the author's group and are now commonly accepted as a superior photocatalyst compared to TiO₂ in the UV region. As its excellence, this paper reviewed the recent progress on BiPO₄, specifically on the efforts from the author's group, including the preparation as well as the modification methods involved in the activity enhancement. The description of physical properties and typical degradation pathways of the photocatalyst were also given for better comprehension of the origin of the high activity. Furthermore, as a represented nonmetallic oxyacid photocatalyst, the research of BiPO₄ will offer guidelines for designing effective photocatalysts of the same type for environmental applications.

1. Introduction

Over the past few years, photocatalytic technology, as an advanced oxidation process, has received great attention for environmental remediation.¹⁻³ Unlike the conventional biodegradation or activated carbon adsorption method, photocatalytic technology provides a powerful oxidation process in the removal of non-biodegradable organic contaminants (e.g. dyes, pesticides, surfactants, etc.) by completely converting them into CO₂ and H₂O and thus, no hazardous breakdown products will be left.⁴ Among all the photocatalysts, TiO₂ has been extensively studied due to its stability, nontoxicity and the ability to photodegrade most of the organic pollutants. However, two issues limit the industrial-scale use of TiO₂: one is TiO₂ absorbs photons only in the UV region (below 400 nm); the other one is that TiO₂ inherently has a rapid recombination rate of photogenerated electrons (e⁻) and holes (h⁺) so that its UV activity is not high enough from a viewpoint of practical applications.

To overcome these two drawbacks, many new photocatalytic systems have been developed in the past decades. These photocatalysts, including complex oxides⁶, nitrides⁷ and sulfides⁸, are mostly focused on extending the absorption wavelength to a visible light region (400-800 nm), with a purpose of utilizing a large portion of sunlight. Among them, some Bi-salt based semiconductors, like BiVO₄⁹ and Bi₂WO₆¹⁰, absorbs visible light due to the upward dispersion of the valence band caused by Bi 6s and O 2p antibonding states and are now regarded as one kind of promising visible-light-responsive photocatalysts. Typically, Bi₂WO₆ photocatalyst, reported by us and other groups, exhibited superior photocatalytic activity for the degradation of rhodamine

B (RhB) and methylene blue (MB) under visible light irradiation.¹⁰⁻¹⁵ In spite of these, if only considered the time consuming, visible-light-responsive photocatalyst still needs much longer time for the degradation of the same concentration of pollutants than UV-responsive photocatalysts. For example, to photodegrade 95% percent of 10⁻⁵ mol/L MB needed several hours on Bi₂WO₆ under visible light irradiation (500 W Xe lamp, λ>420 nm),¹⁶ while it took only 25 minutes in a suspension of TiO₂(Degussa, P25) under UV light irradiation (11W Hg lamp, 254 nm).¹⁷ Besides that, the mineralization ability(the ability to completely convert organic pollutants into CO₂ and H₂O) and stable activity in actual complicated situations are also problems for visible-light-responsive photocatalysts due to a weak redox force resulting from the narrow band gap although they are important necessities for the environmental application. For these reasons, there is quite a long way towards practical applications of visible-light-driven photocatalysts. Instead, if taking the environmental application into consideration, the development of UV-responsive photocatalysts with superior activity to TiO₂ is very meaningful as a practical matter. On this point, some UV-responsive photocatalysts have already been reported to exhibit tens of times higher activity for water splitting into H₂ and O₂ than P25(TiO₂), such as NiO/La:NaTaO₃.¹⁸ However they did not exhibit the same level of photocatalytic activity for organic pollutant degradation because the oxidation of pollutants needs to reduce the O₂, while this reduction is designed to be avoided for water splitting photocatalysts. For the photodegradation of organic pollutants, effective photocatalysts with high activity, good stability and low cost are still lack, compared to TiO₂. In this field, the study is mainly focused on the modification of TiO₂ itself.^{1, 5}

BiPO₄ was used for the first time as a photocatalyst by our group in 2010 and has now been regarded as a promising UV-responsive photocatalyst owing to its superior activity to P25 (TiO₂) in some cases.¹⁸ As was reported¹⁸⁻²², BiPO₄ synthesized with a facile hydrothermal method showed 1-2 times higher photocatalytic activity for degradation of organic pollutants (e.g. dyes, phenol, benzene, etc.) than P25 under UV light irradiation. Also no deactivation was observed during the photocatalytic processes. The excellent photocatalytic activity was considered to be the efficient separation of the photogenerated e⁻ and h⁺ originated from an induced effect inherently possessed by oxyacid anions with high negative charges. With respect to these benefits, studies on the practical use of BiPO₄ was further performed by evaluating its activity in the real wastewater²³ and accounting for the economic running cost as well as comparing with TiO₂.²⁴ The current research on BiPO₄ is focusing on further enhancing the UV-responsive activity, extending the absorption wavelength to the visible-light region, verifying the degradation behavior of more types of pollutants and large-scale preparation for industrial uses. Besides BiPO₄ itself, it is also a representative photocatalyst with a nonmetallic oxy-acid structure. Nonmetallic oxy-acid salts have been employed as photocatalysts in recent years, such as Cu₂(OH)PO₄,²⁵ Bi₂SiO₅,²⁶ Bi₂O₂CO₃,²⁷ BiONO₃,²⁸ Fe₅(PO₄)₄(OH)₃·2H₂O²⁹ and Ag₃PO₄.³⁰ Some of them exhibited very high photocatalytic activity. For example, Ag₃PO₄ obtained a quantum efficiency of over 80% at 440 nm for O₂ production although it suffered from a stability problem.³⁰⁻³³ In this sense the study of BiPO₄ will provide some common properties and pave the way for developing highly efficient and stable oxy-acid photocatalysts for environmental remediation.

In this brief review, we focused on the recent progress on BiPO₄ photocatalyst, including results mainly from the author's group, together with other relative works. This review firstly discussed the influence of the crystal and band structure on the photocatalytic activity of BiPO₄. In the following discussion, methods for optimizing the structural parameters such as the particle size, surface area and morphology were presented for achieving higher activity. And then, the process and mechanism for photodegrading typical environmental pollutants on BiPO₄ were described in detail to give a better understanding of the excellent photocatalytic behavior. Finally the review was focused on the modification methods in order to enhance the UV activity and extend the absorption range of BiPO₄, such as doping metal or nonmetal ions, creating surface oxygen vacancies, forming heterojunctions, hybridizing the surface with π -conjugated materials, etc. In addition, the preparation and improvement of BiPO₄ film was also introduced in this part for an extensive application.

2. Physical properties related to the photocatalytic activity

2.1 Crystal forms

BiPO₄ is known to have three crystal forms³⁴: two monoclinic phases (nMBIP, space group: P2₁/n and mMBIP, space group: P2₁/m) and one hexagonal phase (HBIP, space group: P3₁21), as shown in Fig. 1a. In all three crystals, one bismuth atom is surrounded by eight oxygen atoms and one phosphorus atom is surrounded by four oxygen atoms. The factor that determined the symmetry in crystals has been reported to be the distortion of the Bi-O polyhedron and P-O tetrahedron.³⁵ That is to say, a phase transition requires only a small rotation of the polyhedron for a suitable symmetrical arrangement, not a topological change. Therefore, the transitions between BiPO₄ phases can be simply controlled by adjusting the pH or temperature of the reaction.^{34, 36, 37}

The three phases were measured to have similar band gaps and band edge positions, by UV-Vis spectra (Fig. 1b) and the electrochemical method³⁸, respectively. Despite the similar features, the photocatalytic activity of the three crystal forms was quite different when using MB as a model pollutant.³⁸ nMNIP showed the highest activity while HBIP had the lowest activity. After excluding the influence of the surface area, morphology and band gap, the activity difference was attributed to the efficiency of the separation of photogenerated carriers of three phases, which was supported by the corresponding variation in carrier lifetime as deduced from photoluminescence(PL) decay.³⁸ The separation efficiency was supposed to be influenced by an extra dipole moment induced by the distortion of PO₄³⁻ group. This relationship between photocatalytic activities and dipole moments in BiPO₄ phases is shown in Fig. 1c. The analogous effect has previously been demonstrated in Ga₂O₃, antimonates and Zn₂GeO₄ photocatalysts.³⁹⁻⁴¹ In the case of BiPO₄, the Bi-O bonding contains partially ionic characteristics³⁵ so that the dipole moment in the Bi-O polyhedron can't be simply derived from the geometrical structure. Instead, the dipole moment derived from the distorted PO₄ tetrahedron will induce an extra dipole moment in the Bi-O polyhedron, which thus helps the e⁻/h⁺ separation. Notably, the MB here was only a model pollutant to show the general photocatalytic activity. BiPO₄ phases had the same tendency to degrade other organic pollutants, such as 4-chlorophenol (4-CP), methyl orange (MO), benzene, etc.^{38, 42} Since BiPO₄(nMBIP, space group: P2₁/n) showed ten times higher activity than that of the other two, the following discussion will mainly focus on the properties of this phase unless otherwise specified.

Cite this: DOI: 10.1039/c0xx00000x

www.rsc.org/xxxxxx

ARTICLE TYPE

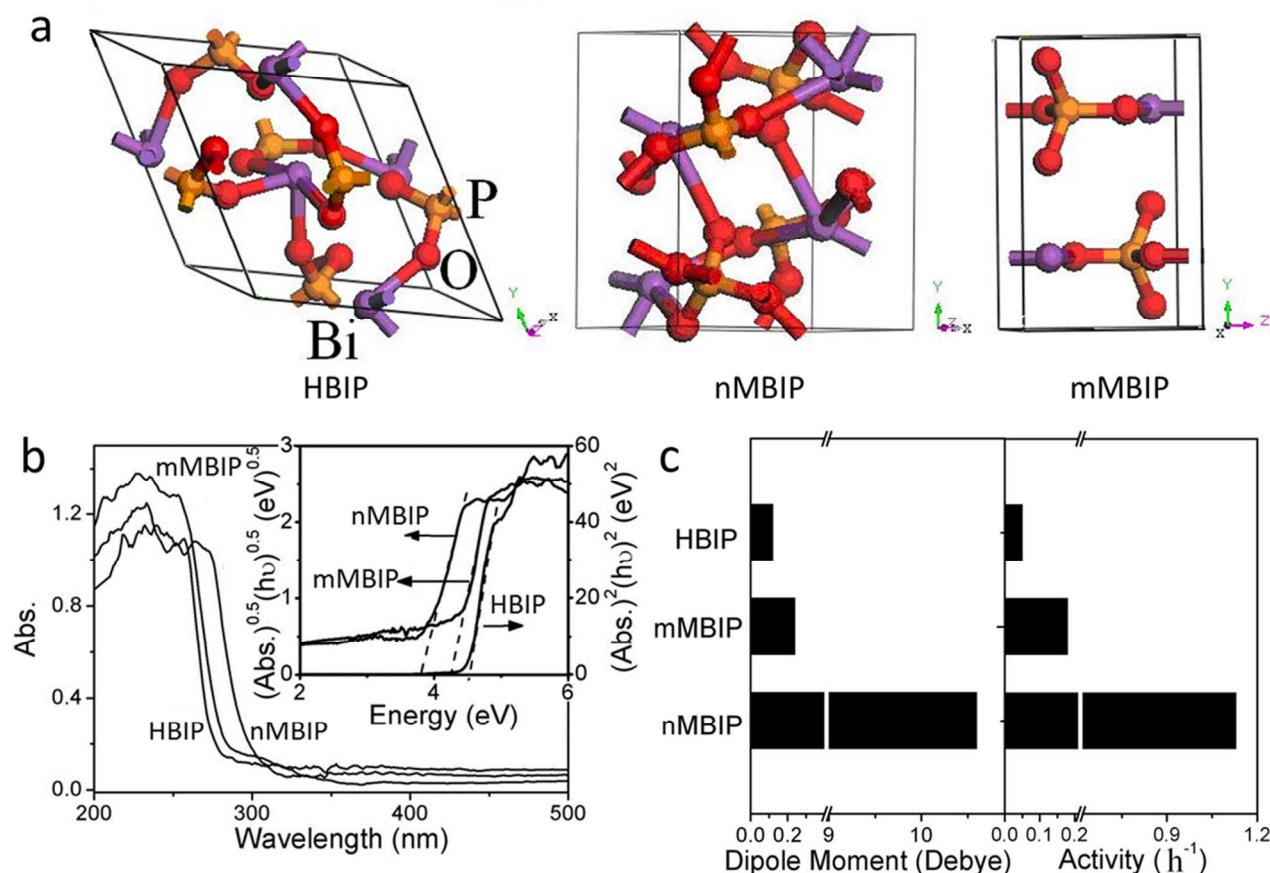


Fig. 1 (a) Structures of different BiPO₄ phases; (b) UV-Vis DRS patterns of various BiPO₄ crystal phases (c) Correlation between dipole moments in various BiPO₄ crystal phases and photocatalytic activities. Reprinted with permission from ref. 38, copyright 2011 Royal Society of Chemistry.

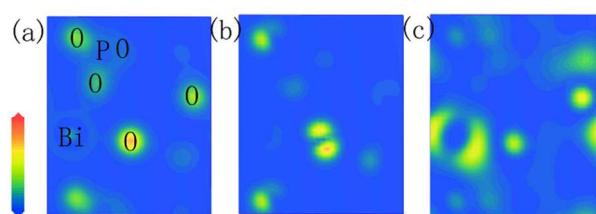


Fig. 2 Charge density contour plots through a plane paralleled to (001) containing both Bi and P atoms: (a) total electron density, (Plotted from 0 (blue) to red 7.00 e·Å⁻³(red)), (b) HOMO, and (c) LUMO. (Plotted from 0 (blue) to red 0.05 (red) e·Å⁻³) Reprinted with permission from ref. 18, copyright 2010 American Chemical Society.

2.2 Band gap and band structure of nMBIP

The band gap of BiPO₄ was reported to be in the range of 3.5–4.6 eV, which could be tuned by the particle size, shape and defects through various synthesis methods.^{20, 43–45} The conduction band minimum (CBM) and valence band maximum (VBM) are located at -0.77 V and 3.08 V, respectively, as determined by the electrochemical method, while at -0.65 V and 3.20 V for each, as calculated by a theoretical method.^{18, 38} In any case, BiPO₄

absorbs only UV light and has a higher VBM potential than that of TiO₂ (2.9 V)⁵, which results in a high oxidation ability. This high oxidation ability is essential for environmental applications as it will provide enhanced mineralization of organic pollutants.

The band structure of BiPO₄ was previously calculated with the program CASTEP as reported by our group.¹⁸ An indirect transition from the VBM to the CBM is observed. The CBM and VBM are consists of the Bi 6p orbitals with a small contribution of the O 2p orbitals and the O 2p orbitals with a small contribution of the Bi 6s orbitals, respectively. This also coincides with the results of other calculations.^{46, 47} A projection of the charge density on (001) surface as shown in Fig.2 showed the advantage of this structure. When a photon excites an electron from O 2p states (HOMO) to Bi 6p states (LUMO) during the photocatalytic process, PO₄³⁻ groups, possessing a large electron cloud overlapping, prefers to attract holes and repel electrons, which helps the e⁻/h⁺ separation. This phenomenon is called the induced effect, described as the action of one group to affect electrostatically the electron density distribution in another group, which is commonly observed in phosphate salts.⁴⁸ Besides that, due to the strong covalency of the P-O bond, PO₄³⁻ ions are

difficult to form oxygen vacancies under ambient conditions.⁴⁹ These oxygen vacancies are considered as recombination centers in TiO₂ or other metal oxide photocatalysts. Also, PO₄³⁻ ions adsorbed on the surface of BiPO₄ may act the same as they did on the TiO₂ surface as reported⁵⁰, such as the strong binding ability with H₂O. These advantages of PO₄³⁻ ions in the structure may result in the superior photocatalytic activity of BiPO₄.

3. Synthesis

Table 1 Synthesis methods and photocatalytic activities of BiPO₄

Methods (Method / Sources / Optimized Conditions)	Products (Morphology/ Mean Size / Surface area/ Bandgap)	Photocatalytic activity (indicated by the apparent kinetics constant, k_{app})	Ref
Hydrothermal Reaction / Na ₃ PO ₄ + Bi(NO ₃) ₃ / pH=1, 180 °C, 72 h	Nanorod / 77×350 nm / 3 m ² g ⁻¹ / 3.85 eV	k_{app} = 0.197 min ⁻¹ for 10 ⁻⁵ M MB, k_{app} = 0.04 min ⁻¹ for 15 ppm 4-CP and k_{app} = 0.184 min ⁻¹ for 10 ⁻⁵ M RhB, (UV-254 11W, cat. 0.5 g/L); as twice as that of P25	18, 20
Hydrothermal Reaction / NaH ₂ PO ₄ + Bi(NO ₃) ₃ / 5% glycerol aq, 160 °C, 24 h	Nanorod / 100×500 nm or Nanoparticle / 35nm / - / 3.85eV	k_{app} = 0.334 min ⁻¹ for 10 ⁻⁵ M MB (UV-254 11W, cat. 0.5 g/L); 1.5 times as high as that prepared by ref. 18	19
Flux / Bi(NO ₃) ₃ +NaH ₂ PO ₄ / pH=2.2, Bi ³⁺ /PO ₄ ³⁻ =1:5, 48 h	Nanorod/ 75×350 nm / 7 m ² g ⁻¹ / 3.85 eV	k_{app} = 0.193 min ⁻¹ (UV-254 11W, 0.5 g/L, 10 ⁻⁵ M MB);	51
Hydrothermal Reaction / NaH ₂ PO ₄ + Bi(NO ₃) ₃ / 160 °C, 24 h	Nanorod / 100×350 nm / 3.7 m ² g ⁻¹ / 3.85 eV	k_{app} = 0.016 min ⁻¹ for 50 ppm phenol(UV-254 11W, cat. 0.5 g/L); Or k_{app} = 0.036 min ⁻¹ by adding 60ppm H ₂ O ₂	52
Microwave synthesis / NaH ₂ PO ₄ + Bi(NO ₃) ₃ / glycerol, EG or DEG aq, 800 W, 15 min	Nanorod (HBIP) / 100×500 nm/ 6.0 m ² g ⁻¹ / 3.88 eV; Nanoneedle (HBIP) / 100 nm×2 μm / 0.5 m ² g ⁻¹ / 3.7eV; Nanoparticle (nMBIP) / 25 nm / 24 m ² g ⁻¹ / 3.6 eV	k_{app} = 0.035 min ⁻¹ for 10 mg/L MO (500 W Xe lamp, cat. 1 g/L)	53
Hydrothermal reaction + Calcination / H ₃ PO ₄ + Bi(NO ₃) ₃ / pH=0, 160 °C, 12 h and then calcined at 750 °C for 2h	Nanorod / 1200×200nm / 4m ² g ⁻¹ / 4.4 eV	Conversion rate 16% for 20 mL/min benzene / O ₂ gas (UV-254 4 W, cat. 0.3 g); as four times as that of P25	47
Hydrothermal reaction + ultrasonic irradiation (20 kHz) / Na ₃ PO ₄ + Bi(NO ₃) ₃ + HNO ₃ / strong sonicated for 30 min and followed by 180 °C, 24 h	Nanorod / 770×155 nm/ 10 m ² g ⁻¹ / 3.8-4.3 eV	k_{app} = ca. 0.15 min ⁻¹ for 5 ppm dyes like triphenylmethyl type (SB, Fast Green FCF) / azo type (MO, OG) / MB (UV-254 10 W); 0.05 min ⁻¹ in real lake water and pond water	23
High-temperature hydrolysis / OA + BEHP + Bi(NO ₃) ₃ / N ₂ , 190 °C, 2 h	Nanocrystal / 9 nm / 75 m ² g ⁻¹ / 4.6 eV	k_{app} = 0.35 min ⁻¹ for 10 ⁻⁵ M MB (UV-254 11W, cat. 0.5 g/L)	46
Solvothermal reaction/ H ₃ PO ₄ + Bi(NO ₃) ₃ + CA-Na / EG-glycerol solution, 120 °C, 20 h	Nanostar constructed by nanorods / 150×10 nm for each rod / - / 3.88 eV	k_{app} = 0.53 h ⁻¹ for 5 ppm RhB and 0.12 h ⁻¹ for 10 ppm MB (UV-254 4 W×6, cat. 1 g/L)	54
Solvothermal reaction/ Na ₃ PO ₄ + Bi(NO ₃) ₃ / EG-water, 160 °C, 4 h	Six-angular microcolumns (HBIP) / 2.7 - × 1.35 μm or Microspindle (nMBIP) / 1.25×0.32 μm / - / -		55
Hydrothermal reaction/ Na ₃ PO ₄ + Bi(NO ₃) ₃ + EDTA / HNO ₃ , 180 °C, 24 h	Six-branch dendrites with high active {002} surface / 30×30 μm / 6.5 m ² g ⁻¹ / 3.5 eV	k_{app} = 0.0294 min ⁻¹ for 10 ⁻⁵ M MB (Xe 500 W, 0.5 g/L, cat.0.8 g/L)	56
Electrospinning method / Bi(NO ₃) ₃ + (NH ₄) ₃ PO ₄ + Citric acid / PVP 0.1 g/mL, pH=1, electrospinning voltage 25 kV, speed 1.5 μm/s	Nanofibers / several centimetres×350 nm/ 25.9 m ² g ⁻¹ / 4.31 eV	k_{app} = 0.01638 min ⁻¹ for 10 ⁻⁵ M APMP pulping effluent (Xe 500W λ≤400 nm, 0.5 g/L, cat. 1.3 g/L) as 3.7 times as that of P25	44

Our group used the hydrothermal method to synthesize BiPO₄, which exhibited nearly twice as high activity for the

The synthesis methods of BiPO₄ were summarized in Table 1. From the Table, hydrothermal synthesis is the main method. By controlling the reaction time, temperature, pH and solvent, BiPO₄ with high activity can be prepared with this method. Other methods like the flux, precipitation-calcination, microwave irradiation and high-temperature hydrolysis are also used to synthesize this material aiming at higher activity.

photodegradation of dyes as P25.¹⁸ By adjusting the reaction temperature (120-180 °C), reaction time (12-96 h) and pH value

(pH=1-7), monoclinic BiPO₄ could be obtained from the ordinary salts of Bi and phosphate, such as Bi(NO₃)₃·5H₂O and Na₃PO₄. If adding glycerol to the reaction mixture, the activity could be further enhanced by 1.5 times.¹⁹ The morphology of BiPO₄ prepared by hydrothermal methods is in most cases a nanorod shape with a mean diameter of 70 nm and a length range from 300 to 1000 nm. The surface area is below 10 m²/g. To increase this surface area, BiPO₄ nanocrystals were also synthesized by a high-temperature hydrolysis method, as reported by our group.⁴⁶ The particle size of BiPO₄ nanocrystals could be controlled from the range of 9 to 200 nm by adjusting the ratio of oleic acid to bis(2-ethylhexyl) phosphate (OA/BEHP). The surface area of a 9 nm nanocrystal reached up to 75 m²/g, which further promoted the activity. Besides the surface area, preparing BiPO₄ with a highly active surface is another way to increase the activity. Recently, Teng et al. reported the synthesis of BiPO₄ dendrites with highly active {002} facets by adding ethylenediaminetetraacetic acid (EDTA) into the hydrothermal system. The activity of the dendrites, under Xe lamp ($\lambda < 420$ nm) irradiation, was enhanced twice as high as BiPO₄ cubes without highly active surfaces exposed. In addition to the activity, a flux method was reported by us to enhance the production of BiPO₄ with a relatively high activity by ten times, with the aim of a large-scale preparation.⁵¹ Except for the improvement of synthesis methods by optimizing the structural parameters, the modification of BiPO₄ with doping, a surface hybridization, a semiconductor combination, and a vacuum treatment can further enhance the activity, which will be discussed in Section 5.

4. Photodegradation process and mechanism of BiPO₄

BiPO₄ is regarded as a new type of photocatalysts as nonmetallic oxy-acid groups like PO₄³⁻ are not conventionally included in the composition of photocatalysts. Since 2010, BiPO₄ has been widely studied due to its excellent photocatalytic activity.¹⁸⁻²³ Up to now, it exhibits high photocatalytic activity for the degradation of typical pollutants that are commonly used in the degradation experiments, as shown in Table 1. The degradation processes is known to follow a pseudo-first-order kinetics model, which is quite common in the photocatalytic system.¹ In Table 1, the activity described by the kinetic rate constants is strongly influenced by the factors including the nanostructure, surface area, light source and the properties of the substrate. The relationship can be fully comprehended by the study of the photodegradation process and mechanism as discussed below.

4.1 Photodegradation of organic pollutants

The photocatalytic activity of BiPO₄ was first demonstrated by degrading dyes and naturally, the following studies were mainly focused on it, including cationic dyes (e.g. MB, RhB) and anionic dyes (e.g. MO).¹⁸ The degradation of dyes is the most common model to evaluate the photocatalytic activity. Dye molecules generally possess a complicated π -conjugated unit acting as a chromophore and the removal of them from textile wastewater by photocatalytic technology is a hot topic. Although the decolorization can be easily observed in the initial stage of photocatalysis, the complete mineralization of dyes needs more than ten times as long for most of the photocatalysts. In the case

of BiPO₄, the decolorization time was comparable to the mineralization time, as monitored by the UV-Vis spectrum and total organic carbon (TOC) analyzer, respectively. That is because the wide band gap and high VBM potential of BiPO₄ could provide a strong oxidation ability to completely convert dyes into CO₂ and H₂O. Not only dyes with a large π -conjugated structure but also small molecular pollutants with single benzene ring like phenol and 4-CP were also reported to be photodegraded and mineralized on BiPO₄. In addition to the liquid phase, it was demonstrated BiPO₄ acted as an effective and stable photocatalyst towards the degradation of volatile organic compounds such as benzene in the gas phase. Wang et al.⁴⁷ reported that BiPO₄ showed three times higher photocatalytic activity for the benzene degradation than P25, due to the ability of the complete mineralization of the pollutants. This mineralization ability avoided the irreversible deactivation derived from the carbonization of the incomplete mineralization. Besides above, some other pollutants were also reported to be photocatalytically degraded by BiPO₄, such as carbamazepine (an example of pharmaceuticals)²¹, dibenzothiophene (a typical pollutant in the photocatalytic oxidative desulfurization)⁵⁷ and alkaline peroxide mechanical pulping (APMP) effluent⁴⁴. In all cases, it exhibited a superior activity to TiO₂(P25) under UV light irradiation.

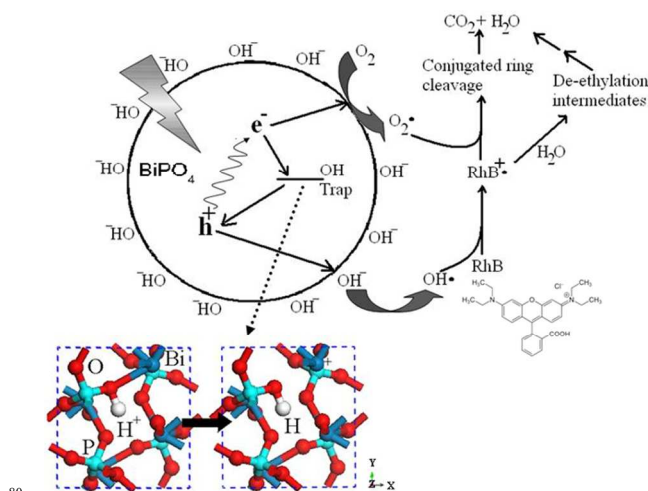


Fig.3 Mechanism of the OH-defects in BiPO₄ crystals influencing on the photocatalytic activity. Reprinted with permission from ref. 20, copyright 2012 Elsevier.

The degradation pathways and mineralization ability were further confirmed to be influenced by OH-related defects commonly existed in photocatalysts of this type.²⁰ For instance, our group found that by the high-performance liquid chromatography coupled with mass spectrometry (HPLC-MS) analysis, the deethylation of RhB occurred first in the existence of BiPO₄ with OH-defects, while the cleavage of the conjugated ring of RhB became primarily when using the well-crystallized catalysts.²⁰ This meant that both the photocatalytic activity and mineralization ability became lower for the catalysts with OH-defects. The reason why the existence of OH-related defects in the lattice decreased the photocatalytic activity was that OH-defects not only acted as recombination centers by trapping of carriers, but also led to a decrease of the superoxide radical production, as shown in Fig.3. This conclusion was supported by photo-electrochemical measurements. Furthermore, the decrease

of the superoxide radical production was quantitatively analyzed by using a Nitroblue tetrazolium (NBT, 2.5×10^{-5} mol/L, absorbed at 259 nm) method.²⁰ By this method, it was determined that the production rate for superoxide radicals was 4×10^{-8} mol/min for BiPO₄ with a defect concentration of 6.0×10^{18} cm⁻³, while 2.4×10^{-7} mol/min for the one with a defect concentration of 1.7×10^{16} cm⁻³.

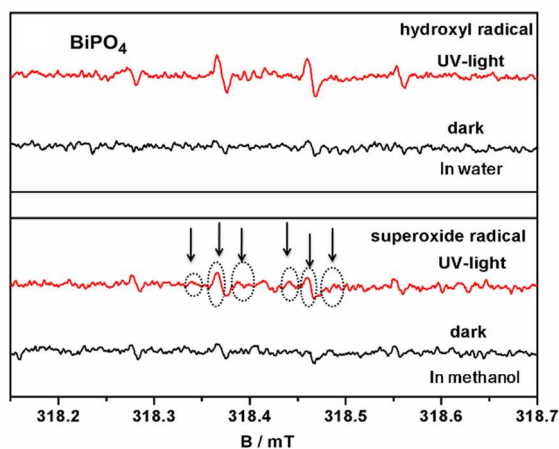


Fig.4 DMPO spin-trapping ESR spectra of BiPO₄ photocatalysts in water and methanol, respectively. Reprinted with permission from ref. 60, copyright 2013 American Chemical Society.

4.2 Active species

The degradation of organic pollutants on BiPO₄ is due to the production of active species during the photocatalytic reaction. Generally speaking, the main active species involved in the photocatalytic process are hydroxyl radicals ($\bullet\text{OH}$), superoxide radicals ($\bullet\text{O}_2^-$) and holes (h^+), respectively.¹ Now the main active species for the photocatalytic reaction on BiPO₄ are determined to be $\bullet\text{OH}$.

The Electron paramagnetic resonance (EPR) technology with trapping experiments has been demonstrated to be effective to identify the active species for the various photocatalysts.⁵⁸⁻⁵⁹ DMPO (5,5-dimethyl-1-pyrroline N-oxide) is a nitron spin trap that converts highly active radicals to some stable adducts, DMPO- $\bullet\text{OH}$ and DMPO- $\bullet\text{O}_2^-$. In the case of BiPO₄ as shown in Fig. 4, the signals of the DMPO- $\bullet\text{OH}$ and DMPO- $\bullet\text{O}_2^-$ (signals with arrows) could be separately observed when conducting the trapping experiments in water and methanol, respectively, and irradiating for 3 min by a Quanta-Ray Nd: YAG pulsed laser system ($\lambda = 270\text{--}410$ nm, 10 Hz).⁶⁰ Further analysis showed that the intensity of $\bullet\text{OH}$ radicals was higher than that of $\bullet\text{O}_2^-$ radicals. Therefore, $\bullet\text{OH}$ radicals not $\bullet\text{O}_2^-$ radicals dominated the photocatalytic process.

The active species trapping experiments were also performed to elucidate the photocatalytic degradation process of BiPO₄.^{18, 60} In a solution with the model pollutant (MB), the photodegradation was slightly suppressed by the addition of a hole scavenger, EDTA⁶¹, while it was obviously inhibited when a hydroxyl radical scavenger, tBuOH⁶¹, was added. Once more, this indicated that the hydroxyl radicals not holes were the main active species to oxidize the adsorbed organic pollutants, which was also reported as the dominantly active ones in TiO₂. In

addition, a degradation experiment in methanol or formate solution was designed to exclude the possibility that $\bullet\text{O}_2^-$ acted as the main active species, based on the fact that $\bullet\text{OH}$ was preferably converted to $\bullet\text{O}_2^-$ in the solution like this.¹⁸

The role of $\bullet\text{OH}$ radicals was further demonstrated by detecting the formation of H₂O₂, as H₂O₂ was known to be the main intermediate products of the $\bullet\text{OH}$ radical reaction.¹ This intermediate product was reported to be measured by an electrochemical method and a spectrophotometric method by adding potassium titanium (IV) oxalate as an indicator, respectively.^{18, 62} In fact, the degradation rate can be significantly enhanced just by adding a small amount of H₂O₂ in the reaction system.

4.3 Degradation pathways and intermediates

Phenol is highly toxic and very difficult to be degraded.⁶³ Here we used it as an example to show how organic pollutants could be degraded on BiPO₄. The formation mechanism of intermediates was analyzed by HPLC-MS and illustrated in Fig. 5. Firstly, photogenerated holes created hydroxyl radicals. These radicals were active to react with phenol to form the hydroquinone (HQ), benzoquinone (p-BQ), catechol and dimer (e.g. 4, 4'-dihydroxybiphenyl). And then, the aromatic ring cleavage occurred to produce carboxylic acids. The carboxylic acids could be directly converted to CO₂ and H₂O by hole oxidation, which thus gave a decrease of the TOC. When adding H₂O₂ into the system as suggested in Section 4.2, the apparent rate constant k was 2.5 times increased, and the mechanism for the enhancement was also shown in Fig.5. Note that H₂O₂ itself enabled the conversion of phenol into its intermediates but was inferior in the complete mineralization compared with the BiPO₄ photocatalyst.

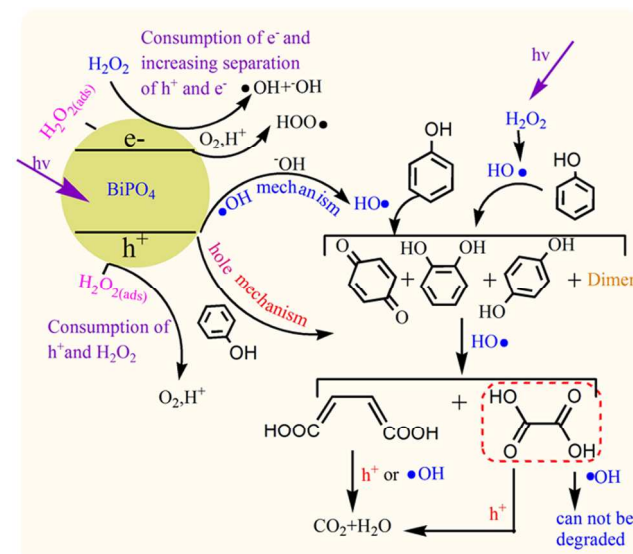


Fig.5 Degradation mechanism of phenol by BiPO₄ and H₂O₂. Reprinted with permission from ref. 52, copyright 2013 Elsevier.

4.4 Selectivity and stability

Selectivity is a very important factor for catalysts. According to the above discussion, the main active species are $\bullet\text{OH}$ radicals. It is well-known that $\bullet\text{OH}$ radicals are almost nonselective and, thus, they will directly react with various organic pollutants due to its high redox potential of 2.7 V vs. NHE.^{1, 5} In Section 4.1, the

superior activity of BiPO₄ to P25 for degrading most of pollutants can therefore be understood: the high activity of BiPO₄ is not due to the special combination of the catalysts to some specific substrates but due to the rapid •OH radical reaction. Although the production of •OH radicals from the photocatalytic reaction of BiPO₄ is almost the same when degrading various pollutants, the degradation pathways differ from each other, which leads to a difference in the photodegradation rate.^{18, 20, 52}

Besides the good photocatalytic activity and non-selectivity, photocatalysts should also display excellent stability during the photocatalytic reaction, which is a key point for practical applications. In fact, the stability problem limits the application of some well-known efficient photocatalysts, like CdS and Ag-based photocatalysts. For BiPO₄, up to now, no experimental data have been reported on the deactivation during the photocatalytic process. Typically, it was reported that during the photodegradation of MB, the catalyst did not exhibit any significant loss of activity after five cycling runs or more, and also the crystal structure was not changed by analyzing the XRD results before and after the reaction.¹⁸ Notably, the adsorption of pollutants on BiPO₄ synthesized by the hydrothermal method was usually small (below 10%) due to the low surface area, which helped to ensure the effective TOC removal and easy recovery of photocatalysts. In a word, BiPO₄ has the high photocatalytic activity to most of the pollutants and stability during the photocatalytic process, which meets the prerequisite for the environmental application.

5. Enhancement of the activity by modification

BiPO₄ is an excellent UV-responsive photocatalyst for the environmental remediation. The high activity is due to the nonmetallic oxyacid structure which is supposed to accelerate the separation of photogenerated charges. Although the activity is rather high compared to P25, UV lamps are needed when BiPO₄ is used in practical situations owing to the wide band gap. This will increase the operating costs. To compensate the cost, further enhancement of the photocatalyst is still needed. Two approaches based on photocatalytic principles have been developed, including: (i) Promoting the separation and transfer of photogenerated charge carriers, (ii) extending the absorption wavelength to the visible light region. At present the modifications that enhance the visible-light photocatalytic activity of BiPO₄ may be more attractive as they can utilize a large portion of sunlight. But in particular, these modifications should not decrease the UV photocatalytic activity at the same time, otherwise the activity under the real sunlight irradiation (UV+Vis) cannot be enhanced.

As discussed in Section 3, the activity of BiPO₄ itself could be enhanced by improving the synthesis methods for optimizing the structural parameters. In this section, the modification methods will be mainly discussed for promoting the activity. These effective modification methods with some of them used to modify TiO₂ include: the doping, formation of the heterojunction structure, surface hybridization, creation of the surface oxygen vacancies and so on.⁶⁴⁻⁹³ By these methods, either the solar light harvesting or charge separation of BiPO₄ has been successfully improved, which thus enhances the photocatalytic activity. The details are shown as follows.

5.1 Doping

The method to introduce nonmetal or metal ions into the structure is well established for TiO₂.^{94, 95} These impurity ions are generally accepted to inhibit the recombination of photogenerated e⁻-h⁺ and decrease the band gap. The main disadvantage is that the doping ions also have a chance to be recombination centers, possibly depending on the dopant species, the concentration, or the doping method, and thus lead to an activity decrease. In the case of BiPO₄, fluorine ions were demonstrated to be an effective dopant by our group.⁶⁴ The F doped BiPO₄ (F-BiPO₄) was synthesized via an in situ fluorination method with NaF as F-source as we previously reported.⁹⁶ The lattice oxygen of BiPO₄ was substituted by the fluorine anion, as demonstrated by the XRD, XPS, UV-Vis DRS and Raman spectra. This substitution resulted in an increased polarizability, which could promote the separation efficiency of e⁻-h⁺ pairs. The photocatalytic activity and mineralization rates of F-BiPO₄ were enhanced by about 30% for the degradation of both MB and phenol when the molar ratio of F/Bi was 0.03 as shown in Fig. 6. Note that F⁻ doping cannot decrease the band gap obviously. An ongoing work showed that S doped BiPO₄ had good UV-light activity and some visible-light activity, with an onset wavelength up to 600 nm. In addition to the S doping, Xie et al prepared P doped BiPO₄ by adding red phosphorus into the hydrothermal system and it showed some visible-light activity for the MB degradation.⁶⁵ On the other hand, due to the active chemical property of BiN, doping N into the crystal lattice of BiPO₄ may be difficult to obtain a stable structure in the ambient conditions.

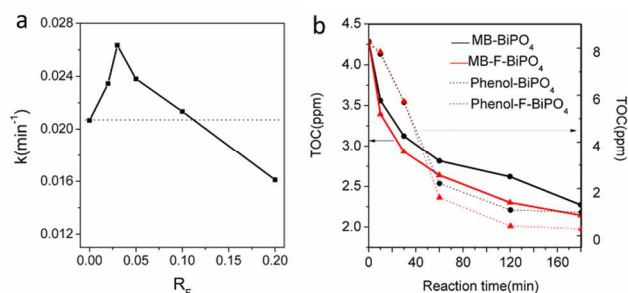


Fig.6 (a) Apparent rate constant (k) for MB degradation vs. R_F (the atomic ratio of F to BiPO₄); (b) Changes of TOC during the photocatalytic degradation of MB and phenol over BiPO₄ and F-BiPO₄ ($R_F=0.03$). Reprinted with permission from ref. 64, copyright 2014 Elsevier.

Besides the nonmetal ions, doping metal ions were also found to be effective for the enhancement of the BiPO₄ photocatalysis. Huang et al. reported that the introduction of Eu³⁺ (1%) or Ga³⁺ (5%) into BiPO₄ lattice by a hydrothermal reaction could increase the activity for the degradation of MB, compared with the undoped one.⁶⁶ In this case, similarly to the F⁻ doping, the band gap was still not changed, remaining at around 4 eV. Other Ln³⁺ doped BiPO₄ was reported as the phosphor material^{97, 98} and some of the doped samples showed the near-UV or visible light absorption but their photocatalytic activity has not yet been studied.

5.2 Heterojunction

Forming heterojunctions between BiPO₄ and another semiconductor or noble metal is an effective way to enhance the activity. As it is well known, most of the photogenerated e⁻ and h⁺

recombined at the surface.⁵ By forming heterojunctions, the photogenerated e^- and h^+ can be efficiently separated at the interface between two semiconductors due to the band alignment or at the one between the noble metal and semiconductor due to the Schottky barrier. Therefore enhancement of the activity can be achieved. Furthermore, the band-edge absorption of another semiconductor or the plasma absorption from the noble metal can extend the absorption wavelength of the photocatalytic system to the visible light region, and thus the composites exhibit visible light activity. This is highly desirable for the practical use of the BiPO_4 photocatalyst.

In the case of the noble metal, loading Ag was reported by Zhang et al. to enhance the UV-light activity of BiPO_4 by four times for the MB degradation under 500 W high-pressure mercury lamp ($\lambda=313$ nm) irradiation.⁶⁷ However, the band-edge adsorption was not extended to the visible region. At this stage, the used BiPO_4 belonged to the nMBIP phase. If incorporating Ag into the lattice of a mixture of nMBIP and mMBIP phases by a sonochemical method, Fulekar et al. reported visible light activity of Ag/ BiPO_4 for the RhB degradation under 150W Xe lamp ($\lambda>400$ nm) irradiation.⁶⁸

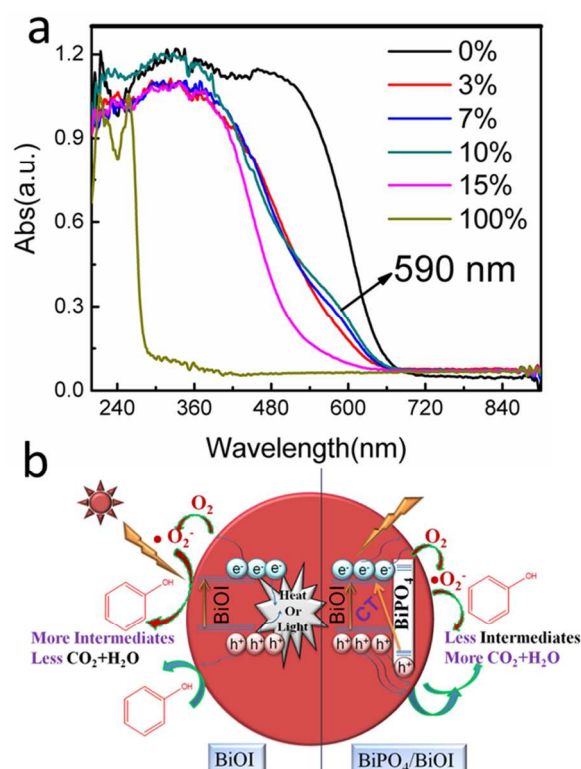


Fig.7 (a) UV-Vis DRS of $\text{BiPO}_4/\text{BiOI}$ with different content of BiPO_4 ; (b) The proposed degradation mechanism of phenol by pure and $\text{BiPO}_4/\text{BiOI}$ composite. Reprinted with permission from ref. 70, copyright 2015 Elsevier.

Besides the noble metal heterojunction, the semiconductor heterojunction can also enable the catalyst to be activated by the visible light. A $\text{BiPO}_4/\text{BiOI}$ composite was reported by us and other groups to be an effective system with promising visible light activity.^{69, 70} In particular, $\text{BiPO}_4/\text{BiOI}$ composite prepared by Liu et al. via an ion-exchange method showed a charge transfer (CT) absorption at ca. 590 nm (Fig. 7a) and due to this absorption, a significant improvement of the visible light activity

was achieved.⁷⁰ That is, under visible light ($\lambda>420$ nm) irradiation, the degradation and TOC removal of phenol on the composite were about 2 and 4 times as high as that on the pure BiOI , respectively. The enhancement of the photocatalytic performance and mineralization ability was attributed to two factors: the increase production of more oxidative holes through the CT process between BiPO_4 donor and BiOI acceptor (Fig. 7b) and the improvement of the separation efficiency of the photogenerated e^- and h^+ by the large dipole moment of BiPO_4 .

Other semiconductor heterojunctions like $\text{AgBr}/\text{BiPO}_4$,⁷¹ $\text{Bi}_2\text{O}_3/\text{BiPO}_4$,⁷² $\text{Bi}_2\text{MoO}_6/\text{BiPO}_4$,⁷³ $\text{BiVO}_4/\text{BiPO}_4$,^{74, 75} CdS/BiPO_4 ,⁷⁶ $\text{Ag}_3\text{PO}_4/\text{BiPO}_4$ ⁷⁷⁻⁸¹ and $\text{Ag}/\text{Ag}_3\text{PO}_4/\text{BiPO}_4$ ⁸² have also been reported to increase the activity either in the UV or visible light region. Among them, the $\text{Ag}_3\text{PO}_4/\text{BiPO}_4$ composite was considered to form a p-n junction so as to exhibit the enhancement of the activity under both the UV and visible light.⁷⁷⁻⁸¹ In addition, the composite showed a more stable activity than Ag_3PO_4 itself due to the acceleration of the charge separation at the surface of Ag_3PO_4 .

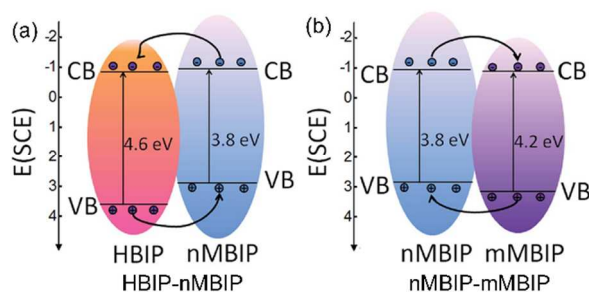


Fig.8 Mechanism for the phase junction. Reprinted with permission from ref. 83, copyright 2014 Royal Society of Chemistry.

5.3 Phase junction

Apart from the above-mentioned heterojunctions, photogenerated e^-h^+ are also known to be efficiently separated by the phase junction, namely, the interface between two different phases of the same material. For example, the mixture of rutile and anatase phases in P25 promotes the separation of photogenerated e^-h^+ due to the band alignment and is thus responsible for the high activity. For BiPO_4 , a similar phase junction was reported by Zhu et al.⁸³ The phase junction was formed by calcining the hexagonal BiPO_4 (HBIP) at different temperatures (350-650 °C). The existence of the phase junction was demonstrated by the HRTEM, XRD and PL-spectra. An nMBIP-mMBIP (94.5 % to 5.5 %) surface-phase junction obtained at 500 °C for 6 h showed the best activity for either the dyes (MO, MB and RhB) or phenol among all the composites. The above phase junction of BiPO_4 further showed 5 times as high as the activity of a macroscopic mixture of the two phases. Interestingly, another phase junction of the HBIP and nMBIP could also be obtained at 400 °C for 6 h, which showed higher activity than the HBIP or nMBIP by themselves. Fig. 8 shows the activity enhancement mechanism for the phase junction. As shown in the scheme, the band edge position of the nMBIP was well matched with the HBIP and mMBIP, and thus the e^-h^+ could be easily separated at the phase junction so that the photocatalytic performance was further improved.

Cite this: DOI: 10.1039/c0xx00000x

www.rsc.org/xxxxxx

ARTICLE TYPE

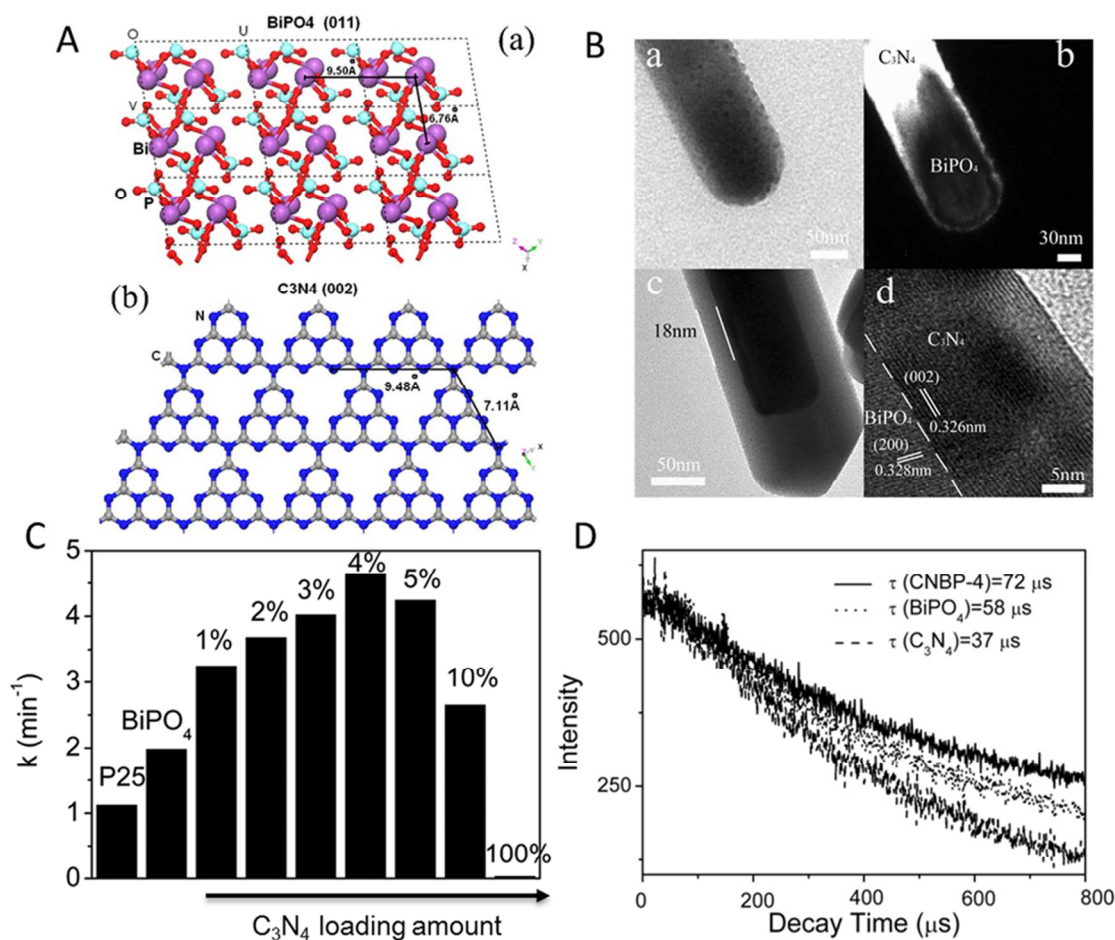


Fig.9 (A) Schematic illustration of the lattice match between (011) surface of BiPO₄ (a) and (002) surface of C₃N₄(b); (B) Bright field TEM (a), dark field TEM (b) and HRTEM images (c, d) of CNBP-10 (10 wt% C₃N₄ loaded BiPO₄); (C) Apparent rate constants for the photodegradation of MB under UV irradiation on C₃N₄/BiPO₄ samples with different weight ratio of C₃N₄ to BiPO₄. BiPO₄, C₃N₄ and P25 were listed as references; (D) aPL decay curves measured at $\lambda_{\text{ex}} = 254 \text{ nm}$ and $\lambda_{\text{em}} = 550 \text{ nm}$ for CNBP-4(4 wt% C₃N₄ loaded BiPO₄), BiPO₄ and C₃N₄. Inset is the lifetime of carriers. Reprinted with permission from ref. 88, copyright 2012 Wiley.

5.4 Surface hybridization with π -conjugated materials

In addition to the metal-semiconductor or semiconductor-semiconductor junctions, a series of the π -conjugated material-semiconductor photocatalyst junctions was reported by the author's group to improve the photocatalytic activity by increasing the separation efficiency of the photogenerated e^-h^+ pairs, such as graphite/TiO₂⁹⁹, C₆₀/ZnO¹⁰⁰, and polyaniline (PANI)/ZnO¹⁰¹. These materials were supposed to be stabilized on the surface of the photocatalysts through a hybridization effect, that is, the interaction between the large π -conjugated system and the electron clouds on the photocatalyst surface. This hybridization effect was already demonstrated to facilitate the charge (the photogenerated e^- or h^+) transfer to the π -conjugated material so as to improve the separation efficiency.⁹⁹⁻¹⁰¹ This modification method was applied on BiPO₄ as well. It was reported that the activity could be significantly enhanced when

BiPO₄ was hybridized with graphene oxide (GO)^{84, 85} and graphene-like carbon nitride (g-C₃N₄)⁸⁶⁻⁸⁸. In most of the case, these composites were not structurally controlled. One special example was g-C₃N₄/BiPO₄.⁸⁸ As we reported previously, a core-shell structured C₃N₄/BiPO₄ photocatalyst was fabricated via a facile ultrasonic dispersion method. The formation of the core-shell structure was due to the match of the crystal faces (Fig. 9A) and illustrated by the HRTEM image in Fig. 9B. The thickness of the shell was controlled by tuning the amount of C₃N₄ in the dispersion, which then influenced the photocatalytic activity. The optimum photocatalytic activity of C₃N₄/BiPO₄ (4 wt% C₃N₄ loaded) under UV light irradiation was nearly 4.5 times as high as that of P25 and 2.5 times of the reported BiPO₄¹⁸. (Fig. 9C) Also, the dramatic visible light activity was induced due to the C₃N₄ ($\lambda_{\text{abs}} < 500 \text{ nm}$) loaded. Under the simulated sunlight irradiation, the apparent rate constant *k* reached up to 0.183 h⁻¹, which was comparable to that of Bi₂WO₆ (0.228 h⁻¹), one of the best visible

light photocatalysts we reported before.¹⁶ The controlled structure along with the matched band position was considered to be effective for the charge separation in $C_3N_4/BiPO_4$ and thus responsible for the enhancement of the performance, which was supported by the longer lifetime of photogenerated carriers in the composites, as measured by the PL-decay spectra (Fig. 9D). When replacing g- C_3N_4 by reduced-GO, a further enhancement was observed by Wang et al.⁸⁴, where the apparent kinetics constant was recorded up to 0.5443 min^{-1} for the MB degradation, that is, nearly 5 times higher than that of P25.

5.5 O vacancies

Another method to enhance the activity and extend the absorption wavelength is to create oxygen vacancies in the $BiPO_4$ structure. An appropriate amount of oxygen vacancies are known to enhance the separation efficiency of the photoinduced carriers and narrow the energy gap by the formation of oxygen vacancy states in the band gap.^{102, 103} In $BiPO_4$, the effects also exist as illustrated in Fig. 10.

In particular, the $BiPO_{4-x}$ nanorod with surface oxygen vacancies was fabricated via the vacuum deoxidation process at $1 \times 10^{-3} - 10^{-4}$ Torr.⁶⁰ The existence of O vacancies was confirmed by the UV-Vis DRS, HRTEM, EPR, Raman and H_2 -TPR. The concentration of O vacancies was then controlled by tuning the deoxidation temperature (110-160°C) and time (1-5h) in vacuum, which thus influence the photocatalytic activity. The optimized photocatalytic activity of the $BiPO_{4-x}$ nanorod (140°C, 3h) was about 1.5 times as high as that of the pure $BiPO_4$. More attractively, the incident photon-to-current conversion efficiency (IPCE) of the $BiPO_{4-x}$ nanorod reached up to 5.5% at 340 nm, and the responsive range was extended to 400 nm. In addition, this kind of $BiPO_{4-x}$ with the surface oxygen vacancies could also be obtained by using a H_2 -reduction reaction. In that case, the optical absorption between 400-800 nm could be obviously increased, indicating a higher oxygen-vacancy concentration.⁸⁹

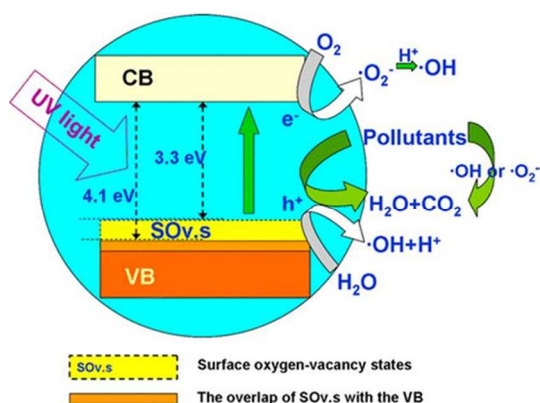


Fig.10 The mechanism of charge separation and photocatalytic reaction of oxygen-vacancy $BiPO_{4-x}$ photocatalyst, under UV light. Reprinted with permission from ref. 60, copyright 2013 American Chemical Society.

Further results showed that the $BiPO_{4-x}$ nanorod had a good stability not only during the photocatalytic degradation but also for the storage. For example, the UV light activity for the degradation of MB on vacancy $BiPO_{4-x}$ showed no obvious loss after five cycling runs and even on the one stored for 10 months more than 95% of the activity was still remained.

5.6 Other modifications of $BiPO_4$ powders

$BiPO_4$ sometimes played a different role in the modification. It was a good dopant in other bismuth-based photocatalysts. Lee et al. reported that doping 0.5% $BiPO_4$ into the $BiVO_4$ lattice could enhance its activity for the O_2 production by 30 times, whereas the activity for the pollutant degradation was not included in their research.⁹⁰ Besides $BiPO_4$ itself, other $BiPO_4$ -based salts were also developed as photocatalysts like Cu_2BiPO_6 , $Na_3Bi_2(PO_4)_3$, $Na_3Bi(PO_4)_2$ and $K_2Bi(PO_4)(MoO_4)$.⁹¹⁻⁹³ Some of them were reported to show the visible light activity. However, the visible light activity was far from satisfied and the UV light activity of them was not as high as that of $BiPO_4$. Nevertheless, it is quite attractive to insert other metal ions into the $BiPO_4$ -based salts for developing a photocatalyst with ideal activity.

5.7 Preparation and modification of the $BiPO_4$ film

The use of a film instead of the powders in the photocatalytic system is another effective way to degrade the pollutants from a technical point of view. The film was also reported to provide a possibility to combine the photocatalytic technology with other advanced oxidation processes like an electro-oxidation method, resulting in a higher efficiency.¹⁰⁴ With this motivation, Lu et al. prepared a $BiPO_4$ film by calcining the amorphous complex precursor film at 550°C on a Ti-substrate.¹⁰⁵ (Fig. 11a) This amorphous complex precursor film was deposited on the Ti-substrate with a dip-coating method from a Bi-P-DTPA complex solution. The thickness of this film is around 200 nm. However due to the different thermal stability of three $BiPO_4$ phases, only an mMBIP film could be obtained. Therefore, it showed relatively low activity for the MB degradation under UV light irradiation, comparing to the TiO_2 film prepared with a similar method. To achieve a higher performance, a graphite-carbon hybridized $BiPO_4$ film was further prepared by controlling the calcination temperature at 400°C. (Fig. 11b) The reaction rate of this film was 1.5 times higher than that of the one prepared at 550 °C. The effect of the graphite-carbon was considered to decrease the recombination of the photogenerated e^-h^+ pairs by scavenging electrons and avoid consuming photogenerated e^- by the peroxy intermediates. (Fig. 11c)

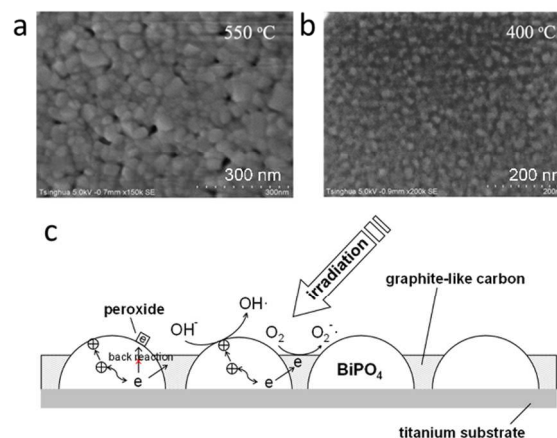


Fig.11 SEM of $BiPO_4$ films (a) and carbon/ $BiPO_4$ film (b) prepared in air under various calcination temperatures, and mechanism for performance enhancement on in-situ carbon hybridized $BiPO_4$ film (c). Reprinted with permission from ref. 105, copyright 2012 Elsevier.

Final remarks

This review article summarized the progress achieved mainly by the author's group on a novel oxyacid photocatalyst, BiPO₄. The monoclinic BiPO₄ (space group: P2₁/n) has now been well accepted as a promising UV-light photocatalyst due to the excellent activity and mineralization ability and in some cases, it showed much higher activity than P25(TiO₂). The superior activity has been suggested to be originated from the induced effect inherently possessed by the nonmetallic oxyacid anions as well as the powerful oxidation ability of holes due to the wide band gap.

In this review, methods with respect to the synthesis optimization and surface modification have been emphasized for further enhancing the activity of BiPO₄. These methods may offer some guideline for improving the photocatalysts with the similar nonmetallic oxyacid structure. In particular, they include: (i) Optimizing synthesis methods can promote the UV-light activity by increasing the surface area and constructing effective structures; (ii) Forming heterojunctions can both enhance the UV-light activity and extend the absorption wavelength, and thus becomes increasingly important; (iii) Hybridizing the surface with π -conjugated materials, like C₃N₄ or r-GO, can achieve the largest enhancement of the activity, that is, around 5 times as high as that of P25.

Based on the presented results, the future research of the BiPO₄ photocatalyst may focus on the following points: (i) the design and synthesis of more effective nanostructures, such as hollow spheres with a high surface area or nanoplates with the highly active surface; (ii) the development of new heterojunctions, e.g. Au/BiPO₄, Pt/BiPO₄, or p-Cu₂O/n-BiPO₄ and the optimization of the present ones, where the heterojunctions may be linked up with the above nanostructures; (iii) the degradation behavior and mechanism of more types of pollutants, especially for non-dyed pollutants; (iv) the preparation of BiPO₄ film with high performance. With the help of future studies on these points, highly efficient BiPO₄ can be expected for the practical use.

Acknowledgements

This work was partly supported by National Basic Research Program of China (973 Program)(2013CB632403), National High Technology Research and Development Program of China (2012AA062701) and Chinese National Science Foundation (21437003 and 21373121).

Notes and references

^aDepartment of Chemistry, Beijing Key Laboratory for Analytical Methods and Instrumentation, Tsinghua University, Beijing, P. R. China Fax: (+86)10-6278-7601; Tel.: (+86)10-6278-3586; E-mail: zhuyf@tsinghua.edu.cn;

- 1 M. R. Hoffmann, S. T. Martin, W. Choi and D. W. Bahnemann, *Chem. Rev.*, 1995, **95**, 69.
- 2 S. Malato, J. Blanco, A. Vidal and C. Richter, *Appl. Catal. B*, 2002, **37**, 1.
- 3 R. Daghrir, P. Drogui and D. Robert, *Ind. Eng. Chem. Res.*, 2013, **52**, 3581.
- 4 C. E. Clarke, F. Kielar, H. M. Talbot and K. L. Johnson, *Environ. Sci. Technol.*, 2010, **44**, 1116.

- 5 J. Schneider, M. Matsuoka, M. Takeuchi, J. Zhang, Y. Horiuchi, M. Anpo and D. W. Bahnemann, *Chem. Rev.*, 2014, **114**, 9919.
- 6 A. Kudo and Y. Miseki, *Chem. Soc. Rev.*, 2009, **38**, 253.
- 7 K. Maeda and K. Domen, *J. Phys. Chem. C*, 2007, **111**, 7851.
- 8 K. Zhang and L. Guo, *Catal. Sci. Technol.*, 2013, **3**, 1672.
- 9 A. Kudo, K. Omori and H. Kato, *J. Am. Chem. Soc.*, 1999, **121**, 11459.
- 10 H. Fu, C. Pan, W. Yao and Y. Zhu, *J. Phys. Chem. B*, 2005, **109**, 22432.
- 11 C. Zhang and Y. Zhu, *Chem. Mater.*, 2005, **17**, 3537.
- 12 L. Zhang, Y. Wang, H. Cheng, W. Yao and Y. Zhu, *Adv. Mater.*, 2009, **21**, 1286.
- 13 H. Fu, L. Zhang, W. Yao and Y. Zhu, *Appl. Catal. B*, 2006, **66**, 100.
- 14 S. Zhang, C. Zhang, Y. Man and Y. Zhu, *J. Solid State Chem.*, 2006, **179**, 62.
- 15 J. Tang, Z. Zou and J. Ye, *Catal. Lett.*, 2004, **92**, 53.
- 16 S. Zhu, T. Xu, H. Fu, J. Zhao and Y. Zhu, *Environ. Sci. Technol.*, 2007, **41**, 6234.
- 17 G. Huang and Y. Zhu, *Mater. Sci. Eng. B*, 2007, **139**, 201.
- 18 C. Pan and Y. Zhu, *Environ. Sci. Technol.*, 2010, **44**, 5570.
- 19 Y. Liu, X. Ma, X. Yi and Y. Zhu, *Acta Phys. Chim. Sin.*, 2012, **28**, 654.
- 20 C. Pan, J. Xu, Y. Chen and Y. Zhu, *Appl. Catal. B*, 2012, **115-116**, 314.
- 21 J. Xu, L. Li, C. Guo, Y. Zhang and W. Meng, *Appl. Catal. B*, 2013, **130-131**, 285.
- 22 L. Wang, J. Tang and H. Yin, *Asian J. Chem.*, 2013, **25**, 2146.
- 23 L. W. Cheng, J. C. Tsai, T. Y. Huang, C. W. Huang, B. Unnikrishnan and Y. W. Lin, *Mater. Res. Express*, 2014, **1**, 025023.
- 24 L. Li, J. Xu, C. Guo and Y. Zhang, *Fron. Environ. Sci. Eng.*, 2013, **7**, 382.
- 25 I. S. Cho, D. W. Kim, S. Lee, C. H. Kwak, S. T. Bae, J. H. Noh, S. H. Yoon, H. S. Jung, D. W. Kim and K. S. Hong, *Adv. Funct. Mater.*, 2008, **18**, 2154.
- 26 R. Chen, J. Bi, L. Wu, W. Wang, Z. Li and X. Fu, *Inorg. Chem.*, 2009, **48**, 9072.
- 27 Y. Zheng, F. Duan, M. Chen and Y. Xie, *J. Mol. Catal. A*, 2010, **317**, 34.
- 28 B. Lu and Y. Zhu, *Phys. Chem. Chem. Phys.*, 2014, **16**, 16509.
- 29 D. Li, C. Pan, R. Shi and Y. Zhu, *CrystEngComm*, 2011, **13**, 6688.
- 30 Z. Yi, J. Ye, N. Kikugawa, T. Kako, S. Ouyang, H. Stuart-Williams, H. Yang, J. Cao, W. Luo, Z. Li, Y. Liu and R. L. Withers, *Nat. Mater.*, 2010, **317**, 559.
- 31 Y. Bi, S. Ouyang, N. Umezawa, J. Cao, and J. Ye, *J. Am. Chem. Soc.*, 2011, **133**, 6490.
- 32 J. Liu, X. Fu, S. Chen, and Y. Zhu, *Appl. Phys. Lett.*, 2011, **99**, 191903.
- 33 S. Kumar, T. Surendar, A. Baruah and V. Shanker, *J. Mater. Chem. A*, 2013, **1**, 5333.
- 34 R. C. L. Mooney-Slater, *Z. Kristallogr.*, 1962, **117**, 371.
- 35 B. Romero, S. Bruque, M. A. G. Aranda and J. E. Iglesias, *Inorg. Chem.*, 1994, **33**, 1869.
- 36 Y. Wang, X. Guan, L. Li and G. Li, *CrystEngComm*, 2012, **14**, 7907.
- 37 S. N. Achary, D. Errandonea, A. Muñoz, P. Rodríguez-Hernández, F. J. Manjón, P. S. R. Krishna, S. J. Patwe, V. Grovera and A. K. Tyagi, *Dalton Trans.*, 2013, **42**, 14999.
- 38 C. Pan, D. Li, X. Ma, Y. Chen and Y. Zhu, *Catal. Sci. Technol.*, 2011, **1**, 1399.
- 39 Y. Hou, L. Wu, X. Wang, Z. Ding, Z. Li and X. Fu, *J. Catal.*, 2007, **250**, 12.
- 40 J. Sato, H. Kobayashi, S. Saito, H. Nishiyama and Y. Inoue, *J. Photochem. Photobiol. A*, 2002, **148**, 85.
- 41 J. Sato, H. Kabayashi, K. Ikarashi, N. Saito, H. Nishiyama and Y. Inoue, *J. Phys. Chem. B*, 2004, **108**, 4369.
- 42 Y. Wang, L. Li, J. Zheng, X. Huang and G. Li, *Chem. Res. Chin. Univ.*, 2013, **29**, 556.
- 43 X. Lin, X. Guo, S. Zhao, X. Gao, H. Zhai, Q. Wang and L. Chang, *Chin. J. Chem. Phys.*, 2014, **27**, 725.
- 44 G. Liu, S. Liu, Q. Lu, H. Sun and Z. Xiu, *Ind. Eng. Chem. Res.*, 2014, **53**, 13023.
- 45 C. Pan and Y. Zhu, *J. Mater. Chem.*, 2011, **21**, 4235.

- 46 Y. A. Hizhnyi, S. G. Nedilko, V. P. Chornii, M. S. Slobodyanik, I. V. Zatonovsky and K. V. Terebilenko, *J. Alloy. Compd.*, 2014, **614**, 420.
- 47 B. Long, J. Huang and X. Wang, *Prog. Nat. Sci.: Mater. Inter.*, 2012, **22**, 644.
- 48 K. Zaghiba, C. M. Julien, *Power Sources*, 2005, **142**, 279.
- 49 C. S. Liu, C. J. Hou, N. Kioussis, S. G. Demos and H. B. Radousky, *Phys. Rev. B*, 2005, **72**, 134110.
- 50 D. Zhao, C. Chen, Y. Wang, H. Ji, W. Ma, L. Zang, J. Zhao, *J. Phys. Chem. C*, 2008, **112**, 5993.
- 51 Y. Zhu, Y. Liu, Y. Lv, H. Wang, Q. Ling and Y. Zhu, *Acta Phys. Chim. Sin.*, 2013, **29**, 576.
- 52 Y. Liu, Y. Zhu, J. Xu, X. Bai, R. Zong and Y. Zhu, *Appl. Catal. B*, 2013, **142-143**, 561.
- 53 G. Li, Y. Ding, Y. Zhang, Z. Lu, H. Sun and R. Chen, *J. Colloid Interface Sci.*, 2011, **363**, 497.
- 54 A. I. Becerro, J. Criado, L. C. Gontard, S. Obregón, A. Fernández, G. Colón and M. Ocaña, *Cryst. Growth Des.*, 2014, **14**, 3319.
- 55 L. Ma, L. Xu, X. Xu, X. Zhou and L. Zhang, *Chem. Lett.*, 2014, **43**, 1306.
- 56 Q. Zhang, H. Tian, N. Li, M. Chen and F. Teng, *CrystEngComm*, 2014, **16**, 8334.
- 57 D. Wang, L. Yue, J. Zhang, M. He, L. Guo and F. Fu, *J. Synth. Cryst. (chn)*, 2014, **43**, 203.
- 58 H. Fu, L. Zhang, S. Zhang and Y. Zhu, *J. Phys. Chem. B*, 2006, **110**, 3061.
- 59 T. Xu, L. Zhang, H. Cheng and Y. Zhu, *Appl. Catal. B*, 2011, **101**, 382.
- 60 Y. Lv, Y. Zhu and Y. Zhu, *J. Phys. Chem. C*, 2013, **117**, 18520.
- 61 L. Zhang and Y. Zhu, *Catal. Sci. Technol.*, 2012, **2**, 694.
- 62 S. Xiong, Y. Fang, X. Li, R. Li and Y. Huang, *Environmental Chemistry(chn)*, 2013, **32**, 1856.
- 63 B. Iurascu, I. Siminiceanu, D. Vione, M. A. Vicente, A. Gil, *Water Research*, 2009, **43**, 1313.
- 64 Y. Liu, Y. Lv, Y. Zhu, D. Liu, R. Zong and Y. Zhu, *Appl. Catal. B*, 2014, **147**, 851.
- 65 J. Xie, W. Wei, H. Cui, G. Chen, R. Liu and S. Zong, *Cn. Pat.*, CN201410235679, 2014.
- 66 H. Huang, H. Qi, Y. He, N. Tian and Y. Zhang, *J. Mater. Res.*, 2013, **28**, 2977.
- 67 Y. Zhang, H. Fan, M. Li and H. Tian, *Dalton Trans.*, 2013, **42**, 13172.
- 68 M. H. Fulekar, A. Singh, D. P. Dutta, M. Roy, A. Ballal and A. K. Tyagi, *RSC Adv.*, 2014, **4**, 10097.
- 69 J. Cao, B. Xu, H. Lin and S. Chen, *Chem. Eng. J.*, 2013, **228**, 482.
- 70 Y. Liu, W. Yao, D. Liu, R. Zong, M. Zhang, X. Ma and Y. Zhu, *Appl. Catal. B*, 2015, **163**, 547.
- 71 H. Xu, Y. Xu, H. Li, J. Xia, J. Xiong, S. Yin, C. Huang and H. Wan, *Dalton Trans.*, 2012, **41**, 3387.
- 72 Q. Du and G. Lv, *J. Inorg. Mater.*, 2014, **29**, 1204.
- 73 X. Lin, D. Liu, X. Guo, N. Sun, S. Zhao, L. Chang, H. Zhai and Q. Wang, *J. Phys. Chem. Solids*, 2015, **76**, 170.
- 74 S. Wu, H. Zheng, Y. Lian and Y. Wu, *Mater. Res. Bull.*, 2013, **48**, 2901.
- 75 H. Lin, H. Ye, S. Chen and Y. Chen, *RSC Adv.*, 2014, **4**, 10968.
- 76 T. Lv, L. Pan, X. Liu and Z. Sun, *RSC Adv.*, 2012, **2**, 12706.
- 77 H. Lin, H. Ye, B. Xu, J. Cao and S. Chen, *Catal. Comm.*, 2013, **37**, 55.
- 78 S. Wu, H. Zheng, Y. Wu, W. Lin, T. Xu and M. Guan, *Ceram. Int.*, 2014, **40**, 14613.
- 79 U. Sulaeman, H. Pratiwi, A. Riapanitra, P. Iswanto, S. Yin and T. Sato, *Adv. Mater. Res.*, 2014, **911**, 92.
- 80 Y. Ren, X. Li and Q. Zhao, *Chem. J. Chinese Univ.*, 2014, **35**, 2435.
- 81 N. Mohaghegh, M. Tasviri, E. Rahimi and M. R. Gholami, *RSC Adv.*, 2015, **5**, 12944.
- 82 Y. Lv, K. Huang, W. Zhang, B. Yang, F. Chi, S. Ran and X. Liu, *Ceram. Int.*, 2014, **40**, 8087.
- 83 Y. Zhu, Y. Liu, Y. Lv, Q. Ling, D. Liu and Y. Zhu, *J. Mater. Chem. A*, 2014, **2**, 13041.
- 84 C. Wang, G. Zhang, C. Zhang, M. Wu, M. Yan, W. Fan and W. Shi, *J. Colloid Interface Sci.*, 2014, **435**, 156.
- 85 E. Gao and W. Wang, *Nanoscale*, 2013, **5**, 11248.
- 86 Z. Li, B. Li, S. Peng, D. Li, S. Yang and Y. Fang, *RSC Adv.*, 2014, **4**, 35144.
- 87 Z. Li, S. Yang, J. Zhou, D. Li, X. Zhou, C. Ge and Y. Fang, *Chem. Engin. J.*, 2014, **241**, 344.
- 88 C. Pan, J. Xu, Y. Wang, D. Li and Y. Zhu, *Adv. Funct. Mater.*, 2012, **22**, 1518.
- 89 Y. Lv, Y. Liu, Y. Zhu and Y. Zhu, *J. Mater. Chem. A*, 2014, **2**, 1174.
- 90 W. J. Jo, J. W. Jang, K. J. Kong, H. J. Kang, J. Y. Kim, H. Jun, K. P. S. Parmar, and J. S. Lee, *Angew. Chem. Int. Ed.*, 2012, **51**, 3147.
- 91 Y. Yang, Y. Murakami, A. Y. Nosaka and Y. Nosaka, *Adv. Technol. Mater. Mater. Process. J.*, 2007, **9**, 115.
- 92 H. Huang, G. Chen and Y. Zhang, *Inorg. Chem. Comm.*, 2014, **44**, 46.
- 93 H. Huang, G. Chen, S. Wang, L. Kang, Z. Lin and Y. Zhang, *Mater. Res. Bull.*, 2014, **51**, 455.
- 94 J. Zhu, W. Zheng, B. He, J. Zhang and M. Anpo, *J. Mol. Catal. A*, 2004, **216**, 35.
- 95 R. Asahi, T. Morikawa, T. Ohwaki, K. Aoki and Y. Taga, *Science*, 2001, **293**, 269.
- 96 G. Huang and Y. Zhu, *J. Phys. Chem. C*, 2007, **111**, 11952.
- 97 Z. Wang, J. Feng, M. Pang, S. Pan and H. Zhang, *Dalton Trans.*, 2013, **42**, 12101.
- 98 M. Guan, J. Sun, F. Tao and Z. Xu, *Cryst. Growth Des.*, 2008, **8**, 2694.
- 99 L. Zhang, H. Fu and Y. Zhu, *Adv. Funct. Mater.*, 2008, **18**, 2180.
- 100 H. Zhang, R. Zong, J. Zhao and Y. Zhu, *Environ. Sci. Technol.*, 2008, **42**, 3803.
- 101 H. Fu, T. Xu, S. Zhu and Y. Zhu, *Environ. Sci. Technol.*, 2008, **42**, 8064.
- 102 L. Chen, Y. Zhao, J. Luo and Y. Xia, *Phys. Lett. A*, 2011, **375**, 934.
- 103 M. Kong, Y. Li, X. Chen, T. Tian, P. Fang, F. Zheng and X. Zhao, *J. Am. Chem. Soc.*, 2011, **133**, 16414.
- 104 X. Zhao and Y. Zhu, *Environ Sci Technol.*, 2006, **40**, 3367.
- 105 B. Lu, X. Ma, C. Pan and Y. Zhu, *Appl. Catal. A*, 2012, **435-436**, 93.

This review presents the recent progress on an oxyacid-type photocatalysts, BiPO_4 , with the excellent UV-activity for environmental applications.